Toward in Vivo Imaging of Heart Disease Using a Radio labeled Single-Chain Fv Fragment Targeting Tenascin-C

ARTICLE *in* ANALYTICAL CHEMISTRY · NOVEMBER 2011

Impact Factor: 5.64 · DOI: 10.1021/ac202159p · Source: PubMed

analytical chemistry

ARTICLE

pubs.acs.org/ac

Toward in Vivo Imaging of Heart Disease Using a Radiolabeled Single-Chain Fv Fragment Targeting Tenascin-C

Norihiro Kobayashi,[*,†] Kenichi Odaka,[‡] Tomoya Uehara,[§] Kyoko Imanaka-Yoshida,[∥,⊥] Yoshinori Kato,[†] Hiroyuki Oyama,[†] Hiroyuki Tadokoro,[#] Hiromichi Akizawa,[§] Shuji Tanada,[▽] Michiaki Hiroe,[○] Toshimitsu Fukumura,[‡] Issei Komuro,[◆] Yasushi Arano,[§] Toshimichi Yoshida,[∥,⊥] and Toshiaki Irie[‡]

[†]Kobe Pharmaceutical University, 4-19-1, Motoyama-Kitamachi, Higashinada-ku, Kobe 658-8558, Japan

[‡]Molecular Imaging Center, National Institute of Radiological Sciences, 4-9-1, Anagawa, Inage-ku, Chiba 263-8555, Japan

[§]Graduate School of Pharmaceutical Sciences, Chiba University, 1-8-1 Inohana, Chuo-ku, Chiba 260-8675 Japan

[∥]Mie University Matrix Biology Research Center, 2-174 Edobashi, Tsu 514-8507, Japan

[⊥]Department of Pathology and Matrix Biology, Graduate School of Medicine, Mie University, 2-174 Edobashi, Tsu 514-8507, Japan

[#]Department of Bio-Medical Engineering, Tokai University, 317, Nishino, Numazu 410-0395, Japan

[▽]Department of Radiation Oncology and Nuclear Medicine, International University of Health and Welfare, Mita Hospital, 1-4-3, Mita, Minato-ku, Tokyo 108-8329, Japan

[○]Department of Cardiology, National Center for Global Health and Medicine, 1-21-1, Toyama, Shinjuku-ku, Tokyo 162-8655, Japan

[◆]Department of Cardiovascular Medicine, Osaka University Graduate School of Medicine, 2-2, Yamadaoka, Suita, Osaka 565-0871, Japan

Supporting Information

ABSTRACT: Antibodies specific to a particular target molecule can be used as analytical reagents, not only for in vitro immunoassays but also for noninvasive in vivo imaging, e.g., immunoscintigraphies. In the latter case, it is important to reduce the size of antibody molecules in order to achieve suitable in vivo "diagnostic kinetics" and generate higher-resolution images. For these purposes, single-chain Fv fragments (scFvs; M_r < 30 kDa) have greater potential than intact immunoglobulins (~150 kDa) or Fab (or Fab′) fragments (~50 kDa). Our recent observation of enhanced tenascin-C (Tnc) expression at sites of cardiac repair after myocardial infarction prompted us to develop a radiolabeled scFv against Tnc for in vivo imaging of heart disease. We cloned the genes encoding the heavy and light chain variable domains of the mouse anti-Tnc monoclonal antibody 4F10, and combined them to create a single gene. The resulting *scFv-4F10* gene was expressed in *E. coli* cells to produce soluble scFv proteins. scFv-4F10 has an affinity for Tnc ($K_a = 3.5 \times 10^7$ M^{-1}), similar to the Fab fragment of antibody 4F10 ($K_a = 1.3 \times 10^7$ M^{-1}) and high enough to be of practical use. A cysteine residue was then added to the C-terminus to achieve site-specific ^{111}In labeling via a chelating group. The resulting ^{111}In-labeled scFv was administered to a rat model of acute myocardial infarction. Biodistribution and quantitative autoradiographic studies indicated higher uptake of the radioactivity at the infarcted myocardium than the noninfarcted one. Single photon emission computed tomography (SPECT) provided in vivo cardiac images that coincided with the ex vivo observations. Our results will promote advances in diagnostic strategies for heart disease.

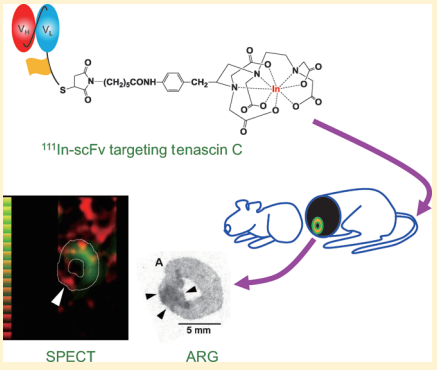

Antibodies, which allow for specific recognition and capture of particular target molecules, have long been used as essential analytical reagents, mainly in the context of in vitro immunoassays and purification systems. Their applications to in vivo diagnostic methods, in which antibodies are administered to patients, are advancing rapidly. By labeling with adequate radioisotopes, antibodies enable powerful in vivo imaging when they are combined with suitable radiation-visualizing instruments. These noninvasive techniques, called immunoscintigraphies, visualize localization and amounts of the distribution of a target molecule in vivo.[1−3]

Most cells are surrounded by an extracellular matrix that functions as a scaffold and is continuously renewed in order to maintain tissue homeostasis. Tenascin-C (Tnc) is a hexameric extracellular matrix glycoprotein.[4−6] Each subunit of the hexamer contains epidermal growth factor (EGF)-like domains and fibronectin type 3 homology repeats (Figure 1). A portion of the fibronectin homology domain is either included or removed

Received: August 24, 2011
Accepted: October 13, 2011
Published: November 10, 2011

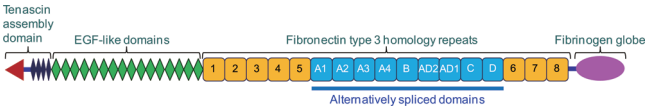

Figure 1. Schematic representation of the molecular structure of one subunit of Tnc.

in the primary transcript on the basis of alternative splicing; this process generates small and large isoforms, which have distinct biological functions.[7,8] While Tnc is highly expressed during embryogenesis, its expression is restricted in normal adult tissues. However, Tnc is reexpressed in tissues undergoing remodeling, inflammatory disease, or cancer invasion. Likewise, Tnc in the heart is observed only in the early stages of embryonic development, not in normal adults. However, the gene is transiently upregulated in association with myocardial injury, e.g., myocardial infarction, ischemia/reperfusion,[9] hibernating myocardium, myocarditis, and some cases of dilated cardiomyopathy (reviewed in ref 10). While Tnc molecules are deposited in the extracellular spaces of diseased hearts, they may also leak into the circulation system. Increased serum levels of Tnc are related to heart disease activity and poorer patient outcome.[11] However, Tnc is not synthesized specifically in the myocardium; therefore, for precise diagnostic purposes, it is necessary to identify the origin of serum Tnc and evaluate the status of cardiac disease using in vivo monitoring and three-dimensional visualization (in vivo imaging) of Tnc expression.

To date, several mouse monoclonal antibodies against Tnc have been generated; some of them have been applied to in vivo targeting of tumors.[12−15] Previously, our group has raised a mouse monoclonal antibody, clone 4F10, which binds to the EGF-like domain of Tnc.[16] Using Fab′ fragment of antibody 4F10 labeled with indium-111 (^{111}In-Fab′), we succeeded in in vivo imaging (single photon emission computed tomography [SPECT]) as well as ex vivo imaging (autoradiography) of inflammatory lesion in the hearts of rat models of myocarditis[17] and myocardial infarction.[18] These results have prompted us to develop advanced in vivo strategies for diagnosing heart disease, using antibody 4F10.

To obtain more suitable behavior in vivo ("diagnostic kinetics"), however, it was necessary to further reduce the size of the Fab fragment.[19,20] Single-chain Fv fragments (scFvs) are antibody fragments produced by genetic manipulation, in which the heavy and light chain variable domains (V_H and V_L, respectively) are combined via flexible peptide linkers.[20−22] Their much smaller molecular mass (<30 kDa) relative to Fab or Fab′ fragments (~50 kDa), attained by removing the constant regions, not only permits deeper penetration into tissues as well as faster clearance from the blood,[23−27] but also might reduce immunogenicity after administration to human patients.[28] Their kinetics might lead to a higher target tissue-to-blood ratio, which in turn would increase the image resolution. Thus, scFvs are expected to be excellent probes for in vivo imaging of Tnc.

SPECT[1−3] is a powerful diagnostic method for visualizing in vivo the three-dimensional localization of molecules that have been labeled with γ-ray-emitting radioisotopes. In this study, we generated an scFv against Tnc (scFv-4F10) by combining the V_H and V_L domains of antibody 4F10. After evaluating its binding affinity, we labeled scFv-4F10 with ^{111}In in a site-specific manner at its C-terminus via a chelating group (Figure 2). We administered the radiolabeled scFv to a rat model of acute myocardial

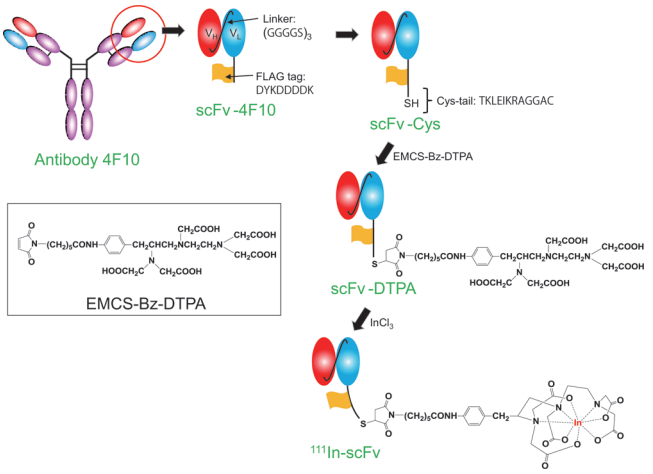

Figure 2. Schematic representation of the preparation of scFv-4F10, introduction of the Cys-tail, conjugation with the DTPA group, and labeling with ^{111}In. The chemical structure of the reagent used for conjugating scFv-4F10 with the chelating group, EMCS-Bz-DTPA, is also shown.

infarction, and observed its distribution by several means including in vivo SPECT imaging, in order to evaluate its utility in monitoring cardiac tissue remodeling.

MATERIALS AND METHODS

Cloning and Sequencing of the Anti-Tnc Antibody *V* genes. The V_H gene fragment was cloned by rapid amplification of cDNA 5′-ends (5′RACE),[29] as described previously.[30] Total RNA was extracted from hybridoma cells (~1 × 10^7) expressing antibody 4F10 (isotypes, γ1 and κ),[16] and reverse transcribed using a mγ1-GSP1 [C_H1(γ1)-specific] primer[30] to produce first-strand cDNA. A poly-dC tail was added to the cDNA, which was then amplified by two-step polymerase chain reaction (PCR). The V_L gene fragment was PCR-amplified using V_L-IIa[31] (nucleotide sequence in Table S1 in the Supporting Information) and mκ-GSP (C_κ-specific) primers.[32] The product obtained was then amplified using V_L-IIa-ext (Table S1 in the Supporting Information) and mκ-GSP primers. Both DNA fragments were gel-purified, ligated into pBluescript II (Toyobo), and transformed into *Escherichia coli* (*E. coli*) XL1-Blue cells (Stratagene).[30,32] Plasmid was extracted from the transformants and sequenced. Because the V_L gene fragment obtained in this manner might have contained a few mutations at its 5′-terminal region due to the use of the degenerate reverse primer (Table S1 in the Supporting Information), the dC-tailed cDNA encoding V_L was amplified separately using V_L-For-(CDR3) primer (Table S1 in the Supporting Information) that hybridizes at the complementarity-determining region (CDR) 3 of the V_L domain, in the combination with AAP[30] primer. The resulting product was amplified again using the same forward primer and AUAP[30] primer; the fragment obtained was subcloned into pBluescript II and sequenced.

Assembly of *scFv-4F10* Gene. The V_H and V_L genes were each PCR-amplified using the first-strand cDNA described above as the template, to add a part of the linker sequence, FLAG tag, and restriction sites.[30,32] The primers used were V_H-Rev1 and V_H-For1 (for V_H) and V_L-Rev1 and V_L-For1 (for V_L), respectively (Table S1 in the Supporting Information). The PCR

conditions were as follows: 35 cycles of 95 °C (1 min), 64 °C (1 min), and 72 °C (2 min), followed by a 10 min extension at 72 °C. The V_H and V_L DNA fragments were gel-purified and spliced by overlap extension PCR as described previously[30,32] but using KOD DNA polymerase (Toyobo).[33]

Expression and Purification of scFv-4F10 Protein. The *scFv-4F10* gene fragment described above was gel-purified and ligated into the *Sfi*I and *Sal*I sites of the pEXmide 5 vector.[32,33] This recombinant plasmid was transformed into nonsuppressor *E. coli* XLOLR cells (Stratagene). A single colony of the transformants was grown and protein expression was induced.[30,32] Next, periplasmic extracts of the cells were prepared,[30,32] and scFv protein contained therein was isolated by affinity chromatography using anti-FLAG M2 affinity gel (Sigma).[33]

Preparation of a DTPA-Conjugated scFv Derivative and Its ^{111}In Labeling. *Introduction of a Cysteine (Cys) Residue at the C-terminus of scFv-4F10. scFv-4F10* gene in the recombinant plasmid was PCR-amplified using V_H-Rev1 and V_L-For2 (containing a Cys codon and double stop codons) primers (Table S1 in the Supporting Information). PCR was carried out using *Ex Taq* DNA polymerase (Takara Bio), with the following conditions: 95 °C (1 min), 60 °C (1 min), and 72 °C (2 min) for 35 cycles, followed by a 10 min extension at 72 °C. The resulting *scFv-Cys* gene fragment was gel-purified, subcloned into pEXmide 5, and transformed into *E. coli* XLOLR cells. scFv-Cys protein expression was induced and purified by affinity chromatography as described above.

Conjugation of scFv with DTPA Group. The affinity-purified scFv-Cys (1.06 mg) in 50 mM sodium phosphate buffer (pH 7.3) (PB; 5.3 mL) was treated with dithiothreitol (final concentration, 50 mM) at 37 °C for 1 h. The mixture was applied to the PD-10 column (GE Healthcare), and the scFv-Cys (960 μg; 34 nmol) was eluted with PB containing 9.0 g/L NaCl (PBS). This was mixed with a solution of a bifunctional chelating agent, EMCS-Bz-DTPA[34] (1.3 mg; 1.9 μmol) in *N,N′*-dimethylformamide (500 μL), incubated at 37 °C for 1 h, and then dialyzed against PBS. The resulting DTPA-conjugated scFv (scFv-DTPA) (380 μg/mL in PBS) was subjected to the assay described below and used for radioisotope labeling.

Assay for Estimating the Introduction of the DTPA Group. scFv-DTPA and unconjugated scFv-Cys (each 50 μg; ∼1.7 nmol) were biotinylated in parallel using a Biotin Labeling Kit-SH (Dojindo Laboratories). The resulting products were subjected to ELISA using Tnc-immobilized microplates (procedure in the Supporting Information), except that peroxidase (POD)-conjugated streptavidin (Jackson ImmunoResearch) was used to monitor bound biotin residues.

^{111}In Labeling of DTPA-Conjugated scFv. The purified scFv-DTPA was labeled with ^{111}In, as previously reported.[35] Briefly, 100 μL of $^{111}InCl_3$ (74 MBq/mL) in 0.02 M HCl was added to a mixed solution (100 μL) of 1.0 M sodium acetate and 1.75 M HCl (4:1). After 3 min, a 200 μL aliquot of scFv-DTPA (0.42 μg/mL) was added, and the reaction mixture was kept at 23 °C for 30 min. Radiochemical purity of the purified product was determined using cellulose acetate electrophoresis.

Acute Myocardial Infarction (MI) Animal Model (MI Rats).[16] Twenty 7-week-old male Wistar rats (Japan SLC) were used for preparation of the animal model. The protocol was approved by the Special Committee on Animal Welfare of the National Institute of Radiological Sciences. The rats were anesthetized with 2.0% isoflurane mixed with 1 L/min room-air gas, underwent tracheotomy, and were ventilated by positive pressure through endotracheal tubes attached to a Harvard small animal respirator (SN-480-5; Shinano). Left thoracotomy was performed, and the left descending coronary artery was ligated. No antibiotic medication was used to prevent allergic inflammation. For all the studies described below, ^{111}In-scFv was administered to these rats 3 days after the surgery.

Biodistribution Study. Eleven MI rats were injected with 25 μg (111 kBq) of ^{111}In-scFv (diluted with nonlabeled scFv-DTPA to adjust radioactivity) dissolved in 300 μL of saline intravenously through the tail vein. At 3 (n = 4), 6 (n = 4), and 24 (n = 3) h after the tracer injection, the MI rats were sacrificed by decapitation under ether anesthesia. Hearts, lung, liver, kidney, spleen, chest (with sutured incision after thoracotomy), hind-limb muscle, stomach, and blood were weighed and then counted for radioactivity using an autowell γ counter (2470 WIZARD; PerkinElmer). To focus on uptake in the infarcted area, the whole heart was divided into infarcted and noninfarcted areas. The infarcted area included white colored muscle and normal colored margin.

Quantitative Autoradiographic and Histopathologic Study. Two MI rats were administered the same dose (740 kBq, 25 μg) of ^{111}In-scFv. Three hours after injection, the hearts were excised and embedded in Tissue-Tek optimum cutting temperature compound (Sakura Finetechnical). Sections of 8 μm thickness were subjected to hematoxylin−eosin staining. For autoradiography, adjacent heart sections of 20 μm thickness were placed in contact with an imaging plate for 4.5 days, and the exposed imaging plate was read using an image analyzer (BAS-1800 system, Fuji film).

In Vivo SPECT Imaging. ^{111}In-scFv in vivo imaging was performed using a dual-isotope SPECT system (GCA 9300A, Toshiba), which consists of a three-headed γ-camera equipped with 1.0-mm pinhole collimators, as described previously.[17] For low- and high-dose experiments, 1.18 (7.97 μg) or 16.4 MBq (111 μg) of ^{111}In-scFv was injected intravenously. To reveal intact heart location, 37 MBq of ^{99m}Tc methoxyisobutyl isonitrile (MIBI) (DRL) was injected intravenously after 21.5 h. At 22 h, the rats were anesthetized with 4.0% isoflurane and maintained in 2.0% isoflurane mixed with 1 L/min room-air gas using a face mask. A 60-min data acquisition was performed at 120 s per view, with stepwise rotation at 4° intervals over 120° and multiple peak acquisition (15% window for ^{99m}Tc and 20% window for ^{111}In). The data acquisition matrix was 128 × 128 pixels, and the pixel size for image display was 0.6 mm.

RESULTS

Cloning and Characterization of the V_H and V_L Domains of Anti-Tnc Antibody 4F10. The V_H and V_L genes of the mouse monoclonal anti-Tnc antibody 4F10, which had previously been developed and determined to bind to the EGF-like domain in Tnc,[16] were cloned and sequenced. The amino acid sequences of the V_H and V_L domains were deduced from these nucleotide sequences, and the CDRs were determined according to the Kabat definition[36] (Figure S1 in the Supporting Information). One amino acid substitution (Val3Leu) that arose due to the use of the degenerate cloning primer (V_L-IIa) was found in the N-terminal region of the V_L domain.

Construction of *scFv-4F10* Gene and Bacterial Expression as Soluble Proteins. The *scFv-4F10* gene was constructed by combining the V_H and V_L genes using overlap extension PCR in the following orientation: 5′-*V_H-linker-V_L-FLAG*-3′.[30,32] This gene was expressed in nonsuppressor *E. coli* XLOLR cells to produce soluble

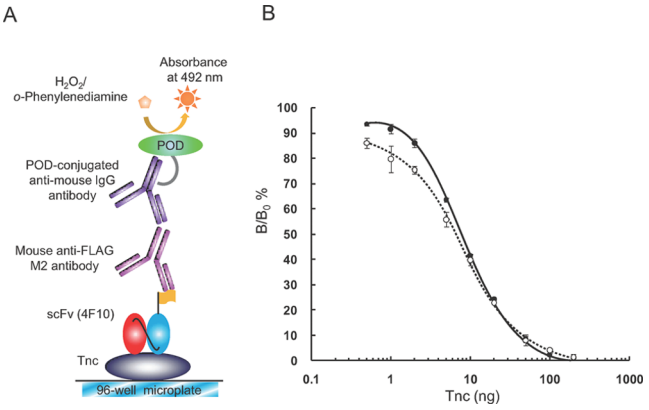

Figure 3. (A) Schematic representation of the competitive ELISA system for examining the Tnc-binding ability of scFv-4F10 and its derivatives. The ELISA procedure is described in the Supporting Information. (B) Dose−response curves of the ELISA for free Tnc using scFv-4F10 (solid line) and scFv-Cys (dotted line). The vertical bars indicate the SD (n = 4).

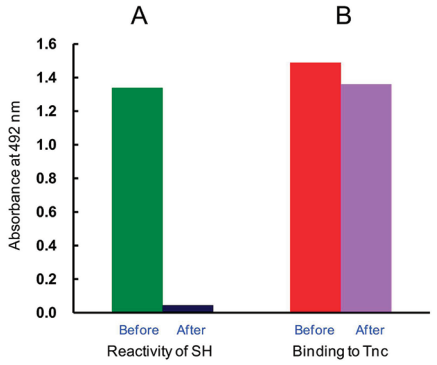

Figure 4. Comparison of (A) the reactivity of SH groups (determined by a SH-specific biotinylation) and (B) the binding activity to Tnc (determined by the ELISA in Figure 3A) of scFv-Cys molecules before and after DTPA conjugation. Details of the procedures are described in the Supporting Information.

scFv protein. The common flexible linker $(Gly_4Ser)_3$[22] was used to connect the V_H and V_L domains, and the FLAG tag[37] was added at the C-terminus. A protein ribbon structure of the scFv was constructed using the SWISS-MODEL Protein Modeling Server (Figure S2 in the Supporting Information). In XLOLR cells, translation of scFv-4F10 should be terminated by the amber codon inserted in the pEXmide 5 vector[30,32] downstream of the *Sal*I cloning site. Thus, scFv-4F10 actually has an additional 18 amino acids (VDKKVEPKSSTKTHTSGG) after the FLAG tag (Figures 2 and S1); consequently, the relative molecular mass of this scFv is calculated to be 29 157.

In sodium dodecyl sulfate−polyacrylamide gel electrophoresis (SDS-PAGE), the affinity-purified scFv-4F10 ran as a single band at the predicted molecular mass (Figure S3A in the Supporting Information). Western blotting using anti-FLAG antibody indicated in-frame expression of the entire scFv molecule (Figure S3B in the Supporting Information). The yield of this scFv from 1 L bacterial culture was estimated as ∼1 mg by ELISA (Figure 3A), using affinity-purified scFv as a standard.

Binding Characteristics of scFv-4F10 against Tnc. The association rate constant (k_a) and dissociation rate constant (k_d) between purified scFv-4F10 and Tnc were determined to be $8.7 \times 10^3\ M^{-1}\ s^{-1}$ and $2.5 \times 10^{-4}\ s^{-1}$, respectively, using surface plasmon resonance (SPR) (experimental procedure in the Supporting Information). From these data, the affinity constant (K_a) was calculated to be $3.5 \times 10^7\ M^{-1}$, which is very similar to that of the Fab fragment of antibody 4F10 (calculated as $1.3 \times 10^7\ M^{-1}$ by the same SPR analysis). This means that neither the Val3Leu amino acid substitution at the V_L domain nor the additional C-terminal residues (described above) reduced the binding affinity. The ability of scFv-4F10 to bind free (not immobilized) Tnc molecules in the liquid phase was confirmed by competitive ELISA (Figure 3A). The addition of free Tnc inhibited the binding of scFv to the microplate, and the midpoint of the dose−response curve (the Tnc amount inhibiting 50% of the initial binding) was 8.5 ng/assay (34 fmol/assay: calculated as 250 kDa monomer) (Figure 3B).

Preparation and Characterization of the scFv-DTPA. To avoid a decrease in the Tnc-binding affinity after radioisotope labeling, we planned site-specific introduction of the chelating group at a position that is remote from the scFv paratope. Therefore, we attached a peptide tail ("Cys-tail") (Figure 2) including a C-terminal cysteine (Cys)[38] to the C-terminus of scFv-4F10, described above. In the competitive ELISA, this scFv-Cys showed a dose−response curve very similar to that of unmodified scFv-4F10; the midpoint was 8.3 ng (Figure 3B). Thus, introduction of the Cys-tail did not reduce the binding affinity of scFv-4F10 and Tnc. Next, a DTPA derivative EMCS-Bz-DTPA (synthesis in the Supporting Information) was coupled with scFv-Cys, taking advantage of the reaction between the sulfhydryl (SH) and maleimide groups (Figure 2). Although the scFv contains four Cys residues besides the introduced C-terminal Cys (Figure S1 in the Supporting Information), they are highly conserved in both V_H and V_L (at the framework regions 1 and 3), and form disulfide bonds and maintain suitable folding of each domain. Therefore, we predicted that only the C-terminal SH group would be reactive, and the major product was the mono-DTPA-substituted molecule at the C-terminus (Figure 2). Successful introduction of the DTPA group was confirmed by monitoring the remaining reactive SH groups of scFv-Cys before and after the DTPA conjugation. These scFvs were reacted simultaneously with a SH-specific biotinylation reagent, and the products were subjected to ELISA using POD-conjugated streptavidin. The dramatic decrease in ELISA signal of the conjugated product (Figure 4A) indicated that the majority of the reactive SH groups had been reacted with the DTPA derivative. The number of incorporated DTPA groups per scFv-Cys molecule was estimated to be 0.8−1.3. This DTPA-conjugated scFv (scFv-DTPA) showed almost the same Tnc-binding activity as unlabeled scFv-Cys, as determined by the ELISA using the POD-labeled anti-FLAG antibody (Figure 4B).

Stability of the scFv-Cys in Rat Plasma. The biochemical stabilities of scFvs in physiological conditions in mammals are not well characterized, and it is possible that these molecules are more labile than native immunoglobulins. Previously, one of the authors (Kobayashi) found that a fusion protein combining an scFv and alkaline phosphatase was rapidly cleaved at the linker peptide between the scFv and the enzyme, even during incubation in a neutral buffer solution: this might reveal high susceptibility to proteolytic digestion.[39] Taking this into account, we incubated the scFv-Cys in rat plasma at 37 °C for various periods and subjected the products to the ELISA system that is shown in

Table 1. Biodistribution of ^{111}In-scFv-4F10 in a Rat Model of MI

	% ID/g[a]		
tissue	3 h[g] (n = 4)	6 h[g] (n = 4)	24 h[g] (n = 3)
blood	0.19 ± 0.09	0.12 ± 0.02	0.04 ± 0.02[e,f]
noninfarcted myocardium	0.08 ± 0.02	0.06 ± 0.01[b]	0.08 ± 0.03
infarcted myocardium	0.17 ± 0.04[c]	0.14 ± 0.05[c]	0.14 ± 0.06[c]
lung	0.14 ± 0.01[c]	0.12 ± 0.01[c,e]	0.16 ± 0.09
liver	4.75 ± 0.45[b,c,d]	4.75 ± 1.06[b,c,d]	3.45 ± 0.13[b,c,d,e]
kidney	10.41 ± 0.92[b,c,d]	11.01 ± 0.66[b,c,d]	8.96 ± 0.63[b,c,d,f]
spleen	1.65 ± 0.18[b,c,d]	1.64 ± 0.28[b,c,d]	1.50 ± 0.22[b,c,d]
stomach	0.94 ± 0.89	0.93 ± 0.44	0.03 ± 0.01
hind-limb skeletal muscle	0.03 ± 0.01[b,c,d]	0.02 ± 0.00[b,c,d,e]	0.02 ± 0.00
chest injury	0.30 ± 0.05[c,d]	0.27 ± 0.01[b,c,d]	0.21 ± 0.06[b,c,d]
infarcted/noninfarcted ratio	2.1 ± 0.2	2.2 ± 0.6	1.9 ± 0.2
infarcted myocardium/blood ratio	1.0 ± 0.3	1.2 ± 0.6	4.4 ± 1.7[e,f]

[a] Values at each time point represent mean ± SD of percentage of injected dose per gram tissue weight (% ID/g) that was calculated as follows: % ID/g = cpm of tissue/cpm of ^{111}In-scFv injected/tissue weight/250 × body weight ×100. Comparisons among three groups were made using the unpaired Student t-test. [b] $P < 0.05$ versus blood. [c] $P < 0.05$ versus noninfarcted area. [d] $P < 0.05$ versus infarcted area. [e] $P < 0.05$ versus rats 3 h after ^{111}In-scFv injection. [f] $P < 0.05$ versus rats 6 h after ^{111}In-scFv injection. [g] Time after ^{111}In-scFv injection.

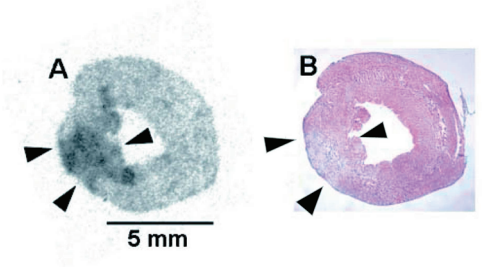

Figure 5. (A) Autoradiography and (B) hematoxylin−eosin staining of adjacent sections from hearts of the acute MI rats. The autoradiography shows heart sections from MI rats to which ^{111}In-scFv had been administered. Accumulation of radioactivity (arrowheads in (A)) was observed in the infarcted lesion area, which appears pale pink due to loss of cardiomyocytes (arrowheads in (B)).

Figure 3A. A slight decrease in the binding activity to Tnc was observed after incubations longer than 2 h. However, ∼70% of the initial activity was retained even after 24 h (Figure S4 in the Supporting Information). These results suggest that scFv-Cys is stable enough for in vivo imaging.

^{111}In Labeling of scFv-DTPA and Preclinical Evaluation for Diagnosing Heart Disease. *^{111}In labeling of scFv-DTPA.* scFv-DTPA was labeled with $^{111}InCl_3$ as described previously.[35] Radiochemical purity of the ^{111}In-scFv obtained was >90%.

Acute Myocardial Infarction Model. No symptoms of infection were seen in the acute MI rats at any time during this study. Five rats died within 30 min of ligation, and two died between 30 min and 1 day after ligation.

Biodistribution of ^{111}In-scFv. Rapid clearance of ^{111}In-scFv from the circulation was inferred from the reduction of radioactivity in the blood. The uptake of radioactivity was the highest in the kidney, followed by liver and spleen. The uptake in the infarcted myocardium was significantly higher than in noninfarcted tissue (Table 1), suggesting that the ^{111}In-scFv specifically bound to the area of the myocardial infarction.

Quantitative Autoradiographic and Histopathologic Study. Via ex vivo autoradiography, high radioactivity was observed in the infarcted lesion of the myocardium (Figure 5A). Histological examination via hematoxylin−eosin staining revealed loss of cardiomyocytes and leukocyte infiltration in the infarcted area (Figure 5). The highest radioactivity in the autoradiographs coincided with the infarcted area (Figure 5). The average level of autoradiographic intensity in the infarcted area was 172.9 photostimulated luminescence (PSL)/mm^2, vs 47.0 PSL/mm^2 in the noninfarcted area. The ratio of autoradiographic intensities of infarcted to noninfarcted areas was 3.68, indicating satisfactory enrichment of ^{111}In-scFv in the infarcted area.

In Vivo SPECT Imaging. Both the low (1.18 MBq; 7.97 μg) and high (16.4 MBq; 111 μg) doses of ^{111}In-scFv revealed accumulation in a region within the infarcted area, which is complementary to the region of adequate myocardial perfusion (Figure 6). Administration of a low dose allowed us to observe heterogeneous myocardial uptake of radioactivity in the infarcted area (Figure 6A). When a higher dose of ^{111}In-scFv was injected, the uptake of radioactivity in myocardium was difficult to distinguish from the high uptake of radioactivity in the liver (Figure 6B).

DISCUSSION

Antibodies and antibody fragments specific to particular biomarker molecules work as excellent probes in clinical diagnoses, not only for in vitro (ex vivo) assays but also for in vivo imaging. While nonisotopic in vivo imaging has recently been developed using fluorochromes emitting near-infrared fluorescence,[3,40,41] radiolabeled antibodies offer robust, reliable, and high-resolution imaging of target molecules, cells, and tissues, especially when used in combination with advanced medical instruments, e.g., SPECT or positron emission computed tomography (PET).

Recently, our group was the first to describe the utility of ^{111}In-labeled anti-Tnc antibody (clone 4F10) and its Fab fragment in the diagnosis of heart disease.[16−18] To achieve in vivo imaging of myocardial injury, myosin is conventionally targeted using radiolabeled anti-myosin antibodies.[42−44] However, targeting of

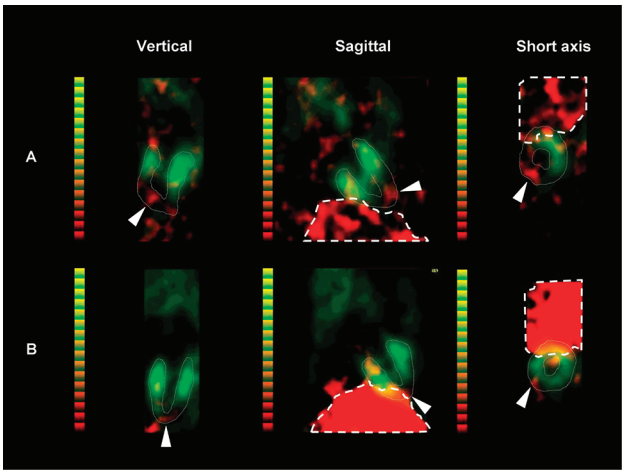

Figure 6. In vivo SPECT imaging obtained after injection of (A) low and (B) high doses of ^{111}In-scFv. Red indicates uptake of ^{111}In-scFv (white arrowheads), and green indicates the uptake of ^{99m}Tc-MIBI, which signifies intact myocardium. The thin white lines show the outline of the myocardium; the thick dotted lines in the sagittal and short axis images show the outline of the liver. Dual-isotope SPECT imaging revealed regional myocardial uptake of ^{111}In-scFv (white arrowheads), which was complementary to the uptake of ^{99m}Tc-MIBI in the MI rats.

Tnc offers advantages over myosin targeting, because it reveals not only injury but also repair of the myocardium; consequently, targeting Tnc enables evaluating the early stages of myocardial remodeling. In this study, in order to gain a more suitable in vivo diagnostic kinetics and possible reduction in the immunogenicity of antibody, we generated an anti-Tnc scFv (scFv-4F10), a much smaller antibody fragment than Fab and Fab′. Another group has reported isolation of an anti-Tnc scFv with 670 nM affinity ($K_a \sim 0.15 \times 10^7$ M^{-1}) from a phage-display antibody library with a human-derived scaffold.[45] In contrast, we cloned V_H and V_L genes of our anti-Tnc antibody 4F10 and combined them to construct the *scFv* gene. The scFv-4F10 obtained exhibited >20-fold higher affinity to Tnc ($K_a = 3.5 \times 10^7$ M^{-1}) relative to the library-derived scFv,[45] and was stable in rat serum during the period required for imaging operations. Next, we linked the DTPA chelating group to the C-terminus of this scFv in a site-specific manner and then labeled with ^{111}In. The DTPA group serves as octadentate ligand to form a stable complex with the $^{111}In^{3+}$ ion[46] (log β of In-DTPA is 28.5 ± 0.08 at 20 °C)[47] (Figure 2), indicating very tight association between the scFv and ^{111}In.

In the biodistribution study in the acute myocardial infarction animal model (the MI rats), we observed significantly higher radioactivity due to ^{111}In-scFv accumulation in infarcted myocardium, where Tnc is expressed for myocardial repair, than in noninfarcted myocardium. The infarcted-to-noninfarcted ratios for the radioactivity were >2.0 at 3 and 6 h after intravenous injection and 1.9 at 24 h after (Table 1). These results suggested that ^{111}In-scFv bound with high specificity to Tnc expressed on the target tissue in vivo, and this binding was stable until 24 h after the injection. Moreover, the quantitative autoradiography clearly showed accumulation of the radioactivity at the infarcted area (Figure 5A).

Compared with our previous studies, in which an ^{111}In-labeled Fab fragment of antibody 4F10 (^{111}In-Fab) was administered to the MI rats,[18] blood clearance of ^{111}In-scFv was significantly faster than that of ^{111}In-Fab, as demonstrated by the lower level of radioactivity remaining in the blood after a specific interval of time (the percentage of the injected dose per gram tissue weight at 6 h after the injection was 0.12 ± 0.02% for ^{111}In-scFv (Table 1) and 0.35 ± 0.03% for ^{111}In-Fab).[18] Comparison with ^{111}In-Fab′, which was administered to the rat models of myocarditis,[17] also supports faster clearance: the percentage in blood at 24 h after the injection was 0.04 ± 0.02% for ^{111}In-scFv (Table 1) and 0.12 ± 0.02% for ^{111}In-Fab′.[17] This faster clearance must be due in part to the smaller molecular size of ^{111}In-scFv and is, being different from the development of therapeutic antibody fragments, a desirable property for diagnostic antibody fragments, because it results in higher target tissue-to-blood signal ratios. In fact, the ratio of radioactivity in infarcted myocardium vs blood reached 4.4 by 24 h after the injection. To obtain a faster response, we might attempt to produce mutated scFv species with an improved association rate constant (k_a) by introducing random point mutations; the scFv-4F10 described here had a somewhat modest k_a value (8.7×10^3 M^{-1} s^{-1}).

High kidney accumulation is a common feature of radiolabeled scFvs,[20] possibly due to scFv excretion and metabolism in the kidney.[48] However, in this study, the uptake of radioactivity by the kidney at 6 h after the injection was significantly lower than in our previous study of ^{111}In-Fab (11.01 ± 0.66% for ^{111}In-scFv and 15.47 ± 1.76% for ^{111}In-Fab).[18] In contrast, accumulation of radioactivity in the liver was slightly higher than for ^{111}In-Fab (4.75 ± 1.06% for ^{111}In-scFv and 3.22 ± 0.30% for ^{111}In-Fab). Since the uptake of ^{111}In-scFv in the spleen (1.64 ± 0.28%) was lower than that of ^{111}In-Fab (2.91 ± 0.67%),[18] it is not likely to be due to higher accumulation of the labeled scFv in macrophages. The smaller scFv may have access to Tnc that is expressed at low levels on the sinusoidal wall of normal liver. The different radioactivity levels in the stomach with time would be attributable to the inclusion of a part of the duodenum that contained radiometabolites excreted from the liver.

In the in vivo imaging of infarcted myocardium using SPECT, we administered two doses of ^{111}In-scFv (7.97 and 111 μg) to the MI rats. The lower dose was estimated to be in the optimal range for the injection of scFvs (5−25 μg) to avoid saturation of the targeted epitopes in the heart, based on our previous study in which we examined the biodistribution of an ^{111}In-labeled anti-Tnc Fab′ fragment in a rat myocarditis model.[17] As expected, the lower dose increased the target-to-background radioactivity ratio and consequently improved the image of the injured area (Figure 6A). The higher dose, which was administered in an attempt to achieve higher contrast, resulted in an unsatisfactory image due to high accumulation of radioactivity in the liver, which overlapped with the heart in images of myocardial uptake (Figure 6B). This undesirable outcome might have been due to saturation of the targeted epitopes in the heart, and subsequent nonspecific accumulation of the excess ^{111}In-scFv.[17]

Thus, applying the scFv described here at a much lower dose than 7.97 μg, after labeling using ^{111}In with much higher specific activity, might further reduce nonspecific accumulation, as shown in a previous report.[49] Higher specific activity might be also achieved by multiple ^{111}In labeling, i.e., introducing multiple DTPA groups into individual anti-Tnc scFv molecules; this might be achieved with a different C-terminal peptide tail containing several Cys residues.

In previous studies, in which whole mouse antibodies were administered to humans,[28,50] the production of human anti-mouse antibodies (HAMA), which have potential adverse effects, has been reported. A radiolabeled human/mouse chimeric

anti-Tnc antibody administered to 25 patients with malignant glioma, however, did not result in a HAMA response.[51] We expect that the scFvs generated in this study will be less immunogenic in humans than the corresponding immunoglobulins or Fab fragments, because the constant regions (heavy and light chains), which induce anti-xenotypic responses, are totally eliminated. Further reducing the size of the scFv described here, e.g., by preparation of corresponding single-domain antibodies that consist of only V_H domains (~15 kDa),[52] might result in even more desirable diagnostic kinetics. Along these lines, a remarkable recent study described an aptamer (29-mer oligoribonucleotide; 13 kDa) that bound to Tnc tightly ($K_d = 5 \times 10^{-9}$ M) enabling imaging of solid tumors with a higher tumor-to-blood ratio than an anti-Tnc antibody (whole immunoglobulin) examined simultaneously.[53]

In conclusion, we generated an scFv that bound to Tnc with sufficiently high affinity to be of practical use. We labeled this molecule with ^{111}In in a site-specific manner, and we propose this radiolabeled scFv as the basis of a novel strategy for diagnosing heart disease, of particular use for in vivo imaging with SPECT. Our ^{111}In-scFv is promising because it accumulates at high levels in infarcted myocardium in a rat model of MI. This ^{111}In-scFv and similar molecules will be useful not only for clinical diagnoses but also for preclinical biomedical studies. Our study also demonstrates the importance of close collaboration between scientists involved in developing immunochemical/radiochemical analytical technologies and advanced clinical diagnostic methods.

■ ASSOCIATED CONTENT

Supporting Information. Additional information as noted in text. This material is available free of charge via the Internet at http://pubs.acs.org.

■ AUTHOR INFORMATION

Corresponding Author

*Telephone: +81-78-441-7548. Fax: +81-78-441-7550. E-mail: no-kobay@kobepharma-u.ac.jp.

■ ACKNOWLEDGMENT

This work was supported in part by a Grant-in-Aid for Scientific Research (Grant 17390342) and a grant for the City Area Program from the Ministry of Education, Culture, Sports, Science and Technology of Japan. We would like to thank Mami Ohnishi, Yasuko Miyanaga, Yukari Tokuhashi, Sayuri Fukushima, Yusuke Hayano, Hitomi Ito, Eri Tanaka, and Shuko Yamaguchi (Kobe Pharmaceutical University) for their assistance in cloning the *scFv* gene, and large-scale expression of the scFv protein. We thank Prof. Carl A. K. Borrebaeck (Lund University, Sweden) and Dr. Eskil Söderlind (Salinator AB, Sweden) for providing the pEXmide 5 vector.

■ REFERENCES

(1) Keane, T. E.; Rosner, I. L.; Wingo, M. S.; McLeod, D. G. *Rev. Urol.* **2006**, *8*, S20–28.

(2) Artiko, V. M.; Sobić-Saranović, D. P.; Krivokapić, Z. V.; Petrović, M. N.; Obradović, V. B. *Neoplasma* **2009**, *56*, 1–8.

(3) Wessels, J. T.; Busse, A. C.; Mahrt, J.; Dullin, C.; Grabbe, E.; Mueller, G. A. *Cytometry, Part A* **2007**, *71A*, 542–549.

(4) Mackie, E. J.; Halfter, W.; Liverani, D. *J. Cell Biol.* **1988**, *107*, 2757–2767.

(5) Erickson, H. P.; Bourdon, M. A. *Annu. Rev. Cell Biol.* **1989**, *5* 71–92.

(6) Koukoulis, G. K.; Gould, V. E.; Bhattacharyya, A.; Gould, J. E.; Howeedy, A. A.; Virtanen, I. *Hum. Pathol.* **1991**, *22*, 636–643.

(7) Murphy-Ullrich, J. E.; Lightner, V. A.; Aukhil, I.; Yan, Y. Z.; Erickson, H. P.; Höök, M. *J. Cell Biol.* **1991**, *115*, 1127–1136.

(8) Borsi, L.; Carnemolla, B.; Nicolò, G.; Spina, B.; Tanara, G.; Zardi, L. *Int. J. Cancer* **1992**, *52*, 688–692.

(9) Taki, J.; Inaki, A.; Wakabayashi, H.; Imanaka-Yoshida, K.; Ogawa, K.; Hiroe, M.; Shiba, K.; Yoshida, T.; Kinuya, S. *J. Nucl. Med.* **2010**, *51*, 1116–1122.

(10) Okamoto, H.; Imanaka-Yoshida, K. *Cardiovasc. Ther.* **2011**, DOI: 10.1111/j.1755-5922.2011.00276.x.

(11) Sato, A.; Aonuma, K.; Imanaka-Yoshida, K.; Yoshida, T.; Isobe, M.; Kawase, D.; Kinoshita, N.; Yazaki, Y.; Hiroe, M. *J. Am. Coll. Cardiol.* **2006**, *47*, 2319–2325.

(12) Balza, E.; Siri, A.; Ponassi, M.; Caocci, F.; Linnala, A.; Virtanen, I.; Zardi, L. *FEBS Lett.* **1993**, *332*, 39–43.

(13) De Santis, R.; Albertoni, C.; Petronzelli, F.; Campo, S.; D'Alessio, V.; Rosi, A.; Anastasi, A. M.; Lindstedt, R.; Caroni, N.; Arseni, B.; Chiodi, P.; Verdoliva, A.; Cassani, G.; Chinol, M.; Paganelli, G.; Carminati, P. *Clin. Cancer Res.* **2006**, *12*, 2191–2196.

(14) Brack, S. S.; Silacci, M.; Birchler, M.; Neri, D. *Clin. Cancer Res.* **2006**, *12*, 3200–3208.

(15) Wang, Y. C.; Zheng, L. H.; Ma, B. A.; Zhou, Y.; Fan, Q. Y. *Hybridoma* **2010**, *29*, 13–16.

(16) Imanaka-Yoshida, K.; Hiroe, M.; Yasutomi, Y.; Toyozaki, T.; Tsuchiya, T.; Noda, N.; Maki, T.; Nishikawa, T.; Sakakura, T.; Yoshida, T. *J. Pathol.* **2002**, *197*, 388–394.

(17) Sato, M.; Toyozaki, T.; Odaka, K.; Uehara, T.; Arano, Y.; Hasegawa, H.; Yoshida, K.; Imanaka-Yoshida, K.; Yoshida, T.; Hiroe, M.; Tadokoro, H.; Irie, T.; Tanada, S.; Komuro, I. *Circulation* **2002**, *106* 1397–1402.

(18) Odaka, K.; Uehara, T.; Arano, Y.; Adachi, S.; Tadokoro, H.; Yoshida, K.; Hasegawa, H.; Imanaka-Yoshida, K.; Yoshida, T.; Hiroe, M.; Irie, T.; Tanada, S.; Komuro, I. *Int. Heart J.* **2008**, *49*, 481–492.

(19) Rodwell, J. D. *Nature* **1989**, *342*, 99–100.

(20) Huhalov, A.; Chester, K. A. *Q. J. Nucl. Med. Mol. Imaging* **2004**, *48*, 279–288.

(21) Bird, R. E.; Hardman, K. D.; Jacobson, J. W.; Johnson, S.; Kaufman, B. M.; Lee, S. M.; Lee, T.; Pope, S. H.; Riordan, G. S.; Whitlow, M. *Science* **1988**, *242*, 423–426.

(22) Huston, J. S.; Levinson, D.; Mudgett-Hunter, M.; Tai, M. S.; Novotńy, J.; Margolies, M. N.; Ridge, R. J.; Bruccoleri, R. E.; Haber, E.; Crea, R.; Oppermann, H. *Proc. Natl. Acad. Sci. U.S.A.* **1988**, *85*, 5879–5883.

(23) Begent, R. H.; Verhaar, M. J.; Chester, K. A.; Casey, J. L.; Green, A. J.; Napier, M. P.; Hope-Stone, L. D.; Cushen, N.; Keep, P. A.; Johnson, C. J.; Hawkins, R. E.; Hilson, A. J.; Robson, L. *Nat. Med.* **1996**, *2*, 979–984.

(24) Larson, S. M.; El-Shirbiny, A. M.; Divgi, C. R.; Sgouros, G.; Finn, R. D.; Tschmelitsch, J.; Picon, A.; Whitlow, M.; Schlom, J.; Zhang, J.; Cohen, A. M. *Cancer* **1997**, *80*, 2458–2468.

(25) Pavlinkova, G.; Beresford, G. W.; Booth, B. J. M.; Batra, S. K.; Colcher, D. *J. Nucl. Med.* **1999**, *40*, 1536–1546.

(26) Batra, S. K.; Jain, M.; Wittel, U. A.; Chauhan, S. C.; Colcher, D. *Curr. Opin. Biotechnol.* **2002**, *13*, 603–608.

(27) Jain, M.; Chauhan, S. C.; Singh, A. P.; Venkatraman, G.; Colcher, D.; Batra, S. K. *Cancer Res.* **2005**, *65*, 7840–7846.

(28) Raynolds, J. C.; Vecchio, S. D.; Sakahara, H.; Lora, M. E.; Carrasquillo, A.; Neumann, R.; Larson, S. M. *Int. J. Radiat. Appl. Instrum., Part B* **1989**, *16*, 121–125.

(29) Frohman, M. A.; Dush, M. K.; Martin, G. R. *Proc. Natl. Acad. Sci. U.S.A.* **1988**, *85*, 8998–9002.

(30) Kobayashi, N.; Ohtoyo, M.; Wada, E.; Kato, Y.; Mano, N.; Goto, J. *Steroids* **2005**, *70*, 285–294.

(31) Nicholls, P. J.; Johnson, V. G.; Blanford, M. D.; Andrew, S. M. *J. Immunol. Methods* **1993**, *165*, 81–91.
(32) Kobayashi, N.; Shibahara, K.; Ikegashira, K.; Shibusawa, K.; Goto, J. *Steroids* **2002**, *67*, 733–742.
(33) Kobayashi, N.; Oyama, H.; Kato, Y.; Goto., J.; Söderlind, E.; Borrebaeck, C. A. K. *Anal. Chem.* **2010**, *82*, 1027–1038.
(34) Xu, H.; Regino, C. A. S.; Bernardo, M.; Koyama, Y.; Kobayashi, H.; Choyke, P. L.; Brechibiel, M. W. *J. Med. Chem.* **2007**, *50*, 3185–3193.
(35) Arano, Y.; Uezono, T.; Akizawa, H.; Ono, M.; Wakisaka, K.; Nakayama, M.; Sakahara, H.; Konishi, J.; Yokoyama, A. *J. Med. Chem.* **1996**, *39*, 3451–3460.
(36) Kabat, E. A.; Wu, T. T.; Perry, H. M.; Gottesman, K. S.; Foeller, C. *Sequences of Proteins of Immunological Interest*; U.S. Department of Health and Human Services, National Institutes of Health; U.S. Government Printing Office: Washington, DC, 1991.
(37) Knappik, A.; Plückthun, A. *Biotechniques* **1994**, *17*, 754–761.
(38) Völkel, T.; Hölig, P.; Merdan, T.; Müller, R.; Kontermann, R. E. *Biochim. Biophys. Acta* **2004**, *1663*, 158–166.
(39) Kobayashi, N.; Iwakami, K.; Kotoshiba, S.; Niwa, T.; Kato, Y.; Mano, N.; Goto, J. *Anal. Chem.* **2006**, *78*, 2244–2253.
(40) Deliolanis, N. C.; Kasmieh, R.; Würdinger, T.; Tannous, B. A.; Shah, K.; Ntziachristos, V. *J. Biomed. Opt.* **2008**, *13*, 044008.
(41) Shcherbo, D.; Shemiakina, I. I.; Ryabova, A. V.; Luker, K. E.; Schmidt, B. T.; Souslova, E. A.; Gorodnicheva, T. V.; Strukova, L.; Shidlovskiy, K. M.; Britanova, O. V.; Zaraisky, A. G.; Lukyanov, K. A.; Loschenov, V. B.; Luker, G. D.; Chudakov, D. M. *Nat. Methods* **2010**, *7* 827–829.
(42) Sikorska, H.; Rousseau, J.; Desputeau, C.; Gervais, A.; Savoie, S.; Ghaffari, M. A.; Bisson, L.; van Lier, J. E. *Int. J. Radiat. Appl. Instrum., Part B* **1990**, *17*, 567–584.
(43) Tamaki, N.; Yamada, T.; Matsumori, A.; Yoshida, A.; Fujita, T.; Ohtani, H.; Watanabe, Y.; Yonekura, Y.; Endo, K.; Konishi, J.; Kawai, C. *J. Nucl. Med.* **1990**, *31*, 136–142.
(44) Yasuda, T.; Palacios, I. F.; Dec, G. W.; Fallon, J. T.; Gold, H. K.; Leinbach, R. C.; Strauss, H. W.; Khaw, B. A.; Haber, E. *Circulation* **1987**, *76*, 306–311.
(45) Silacci, M.; Brack, S.; Schirru, G.; Mårlind, J.; Ettorre, A.; Merlo, A.; Viti, F.; Neri, D. *Proteomics* **2005**, *5*, 2340–2350.
(46) Maecke, H. R.; Riesen, A.; Ritter, W. *J. Nucl. Med.* **1989**, *30* 1235–1239.
(47) Subramanian, K. M.; Wolf, W. *J. Nucl. Med.* **1990**, *31*, 480–488.
(48) Akizawa, H.; Uehara, T.; Arano, Y. *Adv. Drug Delivery Rev.* **2008**, *60*, 1319–1328.
(49) Yui, J.; Hatori, A.; Yanamoto, K.; Takei, M.; Nengaki, N.; Kumata, K.; Kawamura, K.; Yamasaki, T.; Suzuki, K.; Zhang, M. R. *Synapse* **2010**, *64*, 488–493.
(50) Presta, L. G. *Adv. Drug Delivery Rev.* **2006**, *58*, 640–656.
(51) Reardon, D. A.; Quinn., J. A.; Akabani, G.; Coleman, R. E.; Friedman, A. H.; Friedman, H. S.; Herndon, J. E., II; McLendon, R. E.; Pegram, C. N.; Provenzale, J. M.; Dowell, J. M.; Rich, J. N.; Vredenburgh, J. J.; Desjardins, A.; Sampson, J. H.; Gururangan, S.; Wong, T. Z.; Badruddoja, M. A.; Zhao, X.-G.; Bigner, D. D.; Zalutsky, M. R. *J. Nucl. Med.* **2006**, *47*, 912–918.
(52) Muyldermans, S.; Cambillau, C.; Wyns, L. *Trends Biochem. Sci.* **2001**, *26*, 230–235.
(53) Hicke, B. J.; Stephens, A. W.; Gould, T.; Chang, Y.-F.; Lynott, C. K.; Heil, J.; Borkowski, S.; Hilger, C.-S.; Cook, G.; Warren, S.; Schmidt, P. G. *J. Nucl. Med.* **2006**, *47*, 668–678.